

CERENKOV RING IMAGING DETECTOR DEVELOPMENT FOR SLD*

S. WILLIAMS, V. ASHFORD, F. BIRD, D. W. G. S. LEITH,
 T. SHIMOMURA, S. SHAPIRO, A. NUTTALL

Stanford Linear Accelerator Center, Stanford, California, 94305

and

S. YELLIN

University of California, Department of Physics, Santa Barbara, California, 93106

Abstract

Progress in the development of a time projection style photoelectron detector is reported. The development is intended to demonstrate the principles and determine specifications for a practical design of the large CRID device recently described in the SLD design report, wherein a large detector for the Stanford Linear Collider is described. The drift detector utilizes the technique of photo-ionization of Cerenkov light in tetrakis-dimethyl-amino-ethylene (TMAE) vapor at (1700-2200 Å), and drifting the photoelectrons ten's of centimeters to a proportional chamber picket fence, where the drift time provides one coordinate and the wire number the other coordinate. Results are reported on the drifting of photoelectrons from the Cerenkov light and a light pulser over distances of 10 to 60 centimeters.

1. Introduction

Cerenkov-ring-imaging promises to be a very effective method of particle identification in colliding beam physics and has been chosen as the method of identification for the new SLD spectrometer at the Stanford Linear Collider. The technique was chosen because of its superior performance over a large momentum range when compared to other types of particle identification. This is largely due to the new dual radiator approach taken here.

The principle of Cerenkov-ring-imaging was first put forward by Arthur Roberts¹ and was recently reintroduced by the practical proposal from Ypsilantis and Seguinot.² The SLD design has evolved from many discussions with them about their work. Other designs have now been adapted to several quite different experimental geometries.³

A quarter cross section view of the SLD detector is shown in Fig. 1 and a more detailed cross-section of the CRID device is shown in Fig. 2. Particles emerging from the interaction first pass through the vertex and tracking detectors before entering the CRID. The trajectory first takes it through a thin layer of the liquid radiator (C6-F14, perfluoro-n-hexane) whose index of refraction is 1.277. Cerenkov light is produced in a large cone (up to 53 degrees Cerenkov angle) which becomes a large ring when it intercepts the plane of the detector. The trajectory continues into a region filled with a radiator gas (isobutane) whose index is 1.017. Cerenkov light in this region is produced at an angle of up to 50 milliradians and is imaged by spherical mirrors back down to the detector plane.

* Work supported by the Department of Energy, contract DE-AC03-76SF00515, the National Science Foundation, grant no. 82-11410, and KEK, the National Laboratory for High Energy Physics of Japan.

2. Design Challenges

There are many problems that must be solved in the design of this CRID device:

- Minimizing all sources of aberrations of the Cerenkov circle on the detector plane;
- Developing a large area, high-quantum efficiency photocathode to detect the image of the Cerenkov circle;
- Developing an efficient, single-electron detection system which is immune to regenerative feedback background;
- Keeping all gases, liquids and surfaces clean such that the UV reflectance and transmission are maintained near their maximum value for the life of the experiment;
- Maintaining good control of all fields affecting the drift of the single photoelectrons;
- Signal processing in an environment of small single photoelectron avalanches and very large beam ionization avalanches;
- Pattern recognition;
- Choice and handling of the gas and liquid radiators.

Reported here are some results on the development of the photon drift detector.

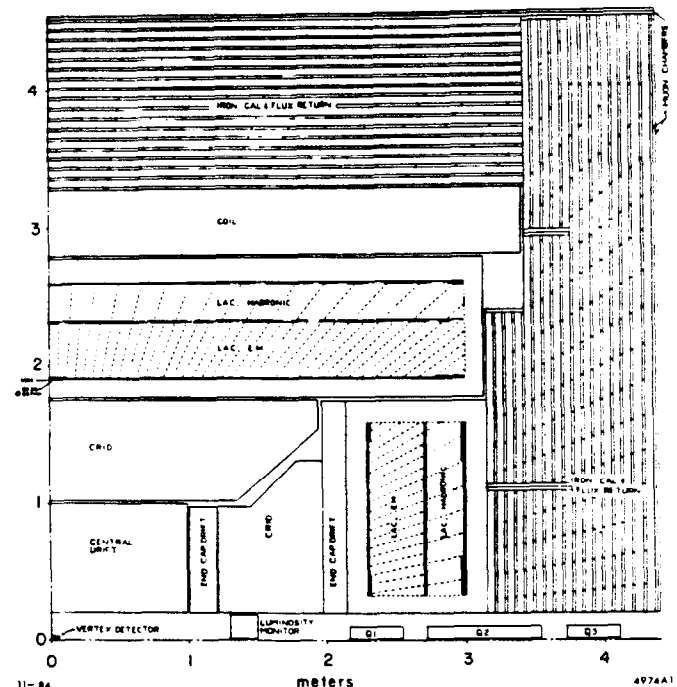


Fig. 1. One-quarter cross-section of the SLD detector at SLC.

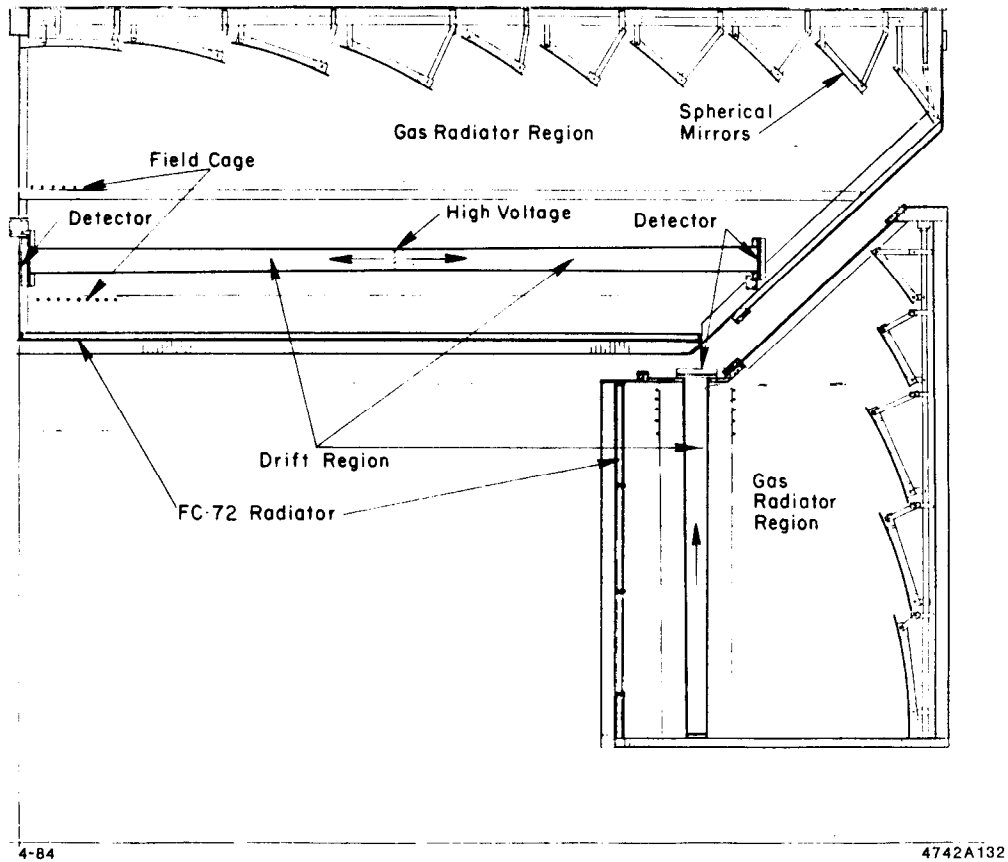


Fig. 2. One-quarter cross-section of the SLD CRID barrel and end cap design.

3. The Photon Detector R & D Status

The photon detector shown in Fig. 2 consists of a 4 centimeter thick box with UV transparent quartz windows on both sides. The Cerenkov photons from the charged particle pass through these windows and are converted by photo-ionization of TMAE vapor, which has a high quantum efficiency in the range 1700 to 2200 Å. The detector box is wound with a field cage establishing an electric drift field along the axis of the detector box, as shown in Fig. 3. The photoelectrons drift at constant velocity down the box until they arrive at the detector, which is a picket fence of multi-wire proportional counters with opaque, conducting blinds between cells. The coordinates of the point of origin of the photoelectron are recorded as the drift time of the electron and the wire address at which the electron was counted.

4. Ring Images

Cerenkov ring images have been observed with a short 20 centimeter drift box built in the described manner and illustrated in Fig. 4 along with the beam line experimental layout. Ring images were obtained from a liquid radiator placed very close to the drift box in order to contain most of the image (although some was still lost due to the large Cerenkov angle from 11 GeV/c pions). Figure 5 shows a radius plot of single photoelectrons from many tracks after radiator-empty data has been subtracted. The right hand slope from 5 to 7 centimeters results from the 11 millimeter absorption length of the TMAE vapor. This effect will be removed when the conversion depth coordinate is read out using charge division on the anode or cathode of the picket fence detector. In an effort to measure N_0 , the Cerenkov efficiency parameter, the ring images were intention-

ally offset in the short drift detector so that one-quarter of the ring image was in the center of the the detector. The image of approximately 200 beam tracks is shown in Fig. 6. When the number of photoelectrons in the left 90 degree quadrant were counted (and the radiator-out count subtracted), five net photoelectrons per track were seen. With a larger detector which fully covered the Cerenkov ring each ring image would have had an average of 20 photoelectrons detected. This results in an N_0 of 50, similar to the expected value of 50-55.

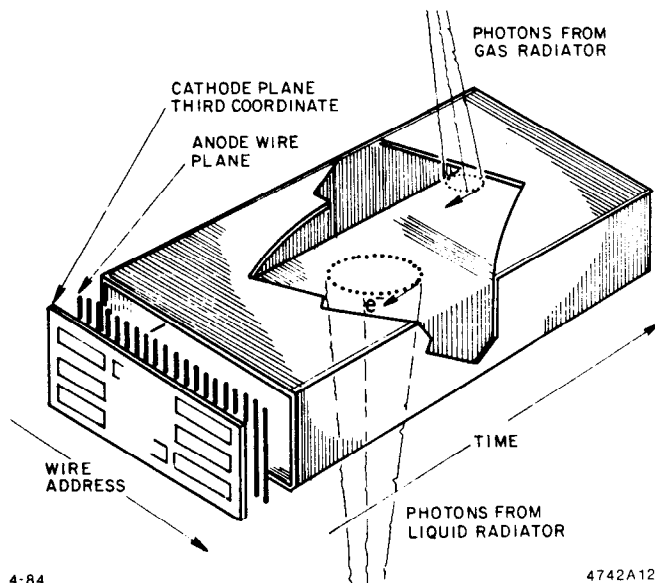


Fig. 3. Photon detector schematic.

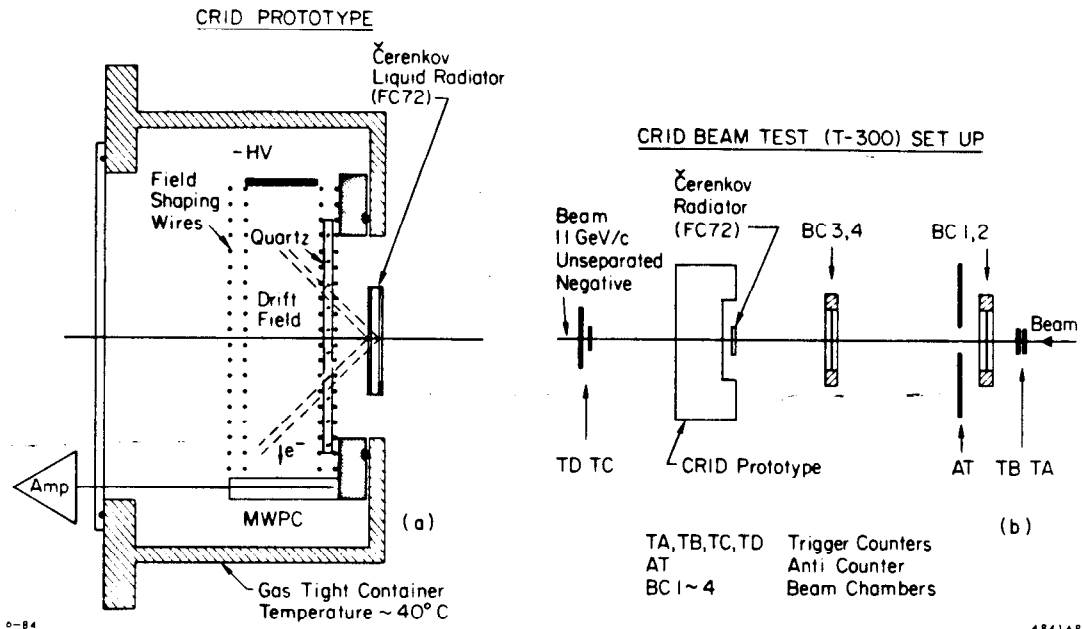


Fig. 4. a) The drift box and Cerenkov radiation cell. (b) The drift box and beam chambers.

5. Long Drift of Single Photoelectrons

The device shown in Fig. 7 has been built to study the problems of drifting Cerenkov rings in a system which has the same essential dimensions as the SLD design. It is built with liquid and gas radiators and a mirror in positions corresponding to the SLD design report, approximately. The long drift box is longer than the longest drift required in the SLD CRID and the entire system is mounted between the pole tips of a magnet capable of exceeding the field specified for the SLD solenoid. The system is in an 11 GeV/c pion or kaon beam at SLAC where it will be studied in late 1984 and 1985. The device has been studied in recent months with a pulsed, focussed nitrogen laser light in order to measure the life-time (and consequently the attenuation-length), and diffusion of single electrons drifting long distances in the detector gas (methane-isobutane). The method involves removal of the mirror and its flange so that a focussed laser spot can be scanned vertically and horizontally over the 20 by 80 centimeter surface of the drift box quartz window.

6. Electron lifetime

The electron lifetime was measured in methane(70%) - isobutane (30%) by focussing the laser spot onto a point in the drift box 60 centimeters away from one wire in the multi-wire picket fence detector. By varying the drift voltage applied to the far end of the drift box, the drift time is varied and recorded by the time-of-flight electronics. The counting rate decreases with increasing drift time as seen in Fig. 8. The lifetime corresponding to the 1/e point is 40 microseconds.

The drift velocity for methane-isobutane results from this measurement and is shown in Fig. 9.

The lifetime was also measured by scanning the laser spot over the length of the drift box at fixed voltage in order to directly measure the loss of photoelectrons versus drift distance. The results shown in Fig. 10 give an attenuation length of 120 cm at 500 V/cm, which corresponds to a lifetime of 34 micro-

seconds for the 70% - 30% mixture with 20 PPM oxygen.

An attempt was made to measure the lifetime of methane without isobutane. The results indicate a lifetime of 75 μ s or longer with 20 PPM oxygen. Since the drift velocity is much higher, 9 cm/ μ s, the attenuation length is much longer, i.e. several meters.

7. Diffusion

Longitudinal diffusion has been studied by looking at the time distribution of electrons from the small laser spot as a function of drift distance. The results are shown in Fig. 11. The value of 180 μ /cm^{1/2} results in a worst case photoelectron resolution of 1.5 mm at 75 cm, the maximum drift distance.

The transverse diffusion is somewhat harder to measure using this apparatus. The technique utilizes the rectangular cell structure of the picket fence detector wires and the smallness of the laser spot (200 microns). It is assumed that the electrostatics of the drift box and picket fence cell results in a zero or 100 per cent chance of detecting the electron on the anode wire depending on whether the electron drifts to the wire or the blind. In the absence of diffusion a scan of the small laser spot across the 4 mm cell would result in a nearly rectangular response curve shown in Fig. 12. Introduction of a gaussian diffusion of the electron as it drifts down the box, will result in a blurring of this sharp profile. Data taken at two drift distances is shown in Fig. 13. The dominance of the diffusion over the intrinsic cell electrostatic width is apparent. The effect of a magnetic field collinear with the electric field was also measured to see if expected shrinkage of the transverse diffusion is significant. The shrinkage is related entirely to the drift velocity, given a fixed electric and magnetic field as follows:

$$\sigma(B) = \frac{\sigma(0)}{\sqrt{1 + \omega^2 \tau^2}} \quad \omega \tau = \frac{B U}{E c}$$

B is the magnetic field (10 kilogauss in SLD, 12.5 kilogauss here), E is the electric field (500 V/cm), and U is the drift velocity.

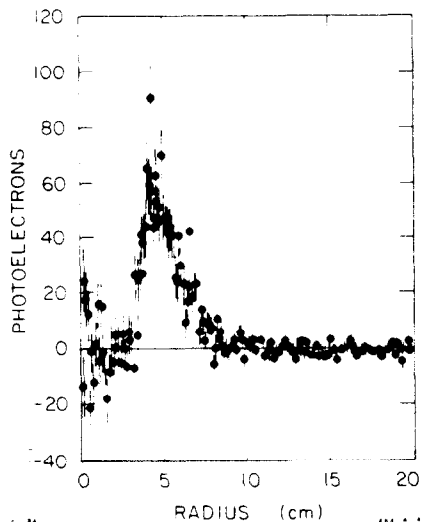
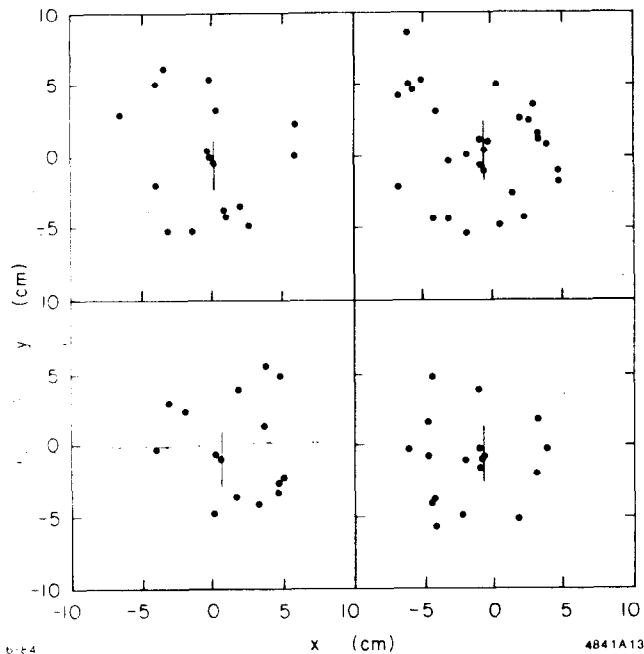


Fig. 5. (a) Ring images made with the apparatus in Fig. 4. (b) Radius projection of x-y residuals for the blinded detector. Radiator-out data was subtracted.

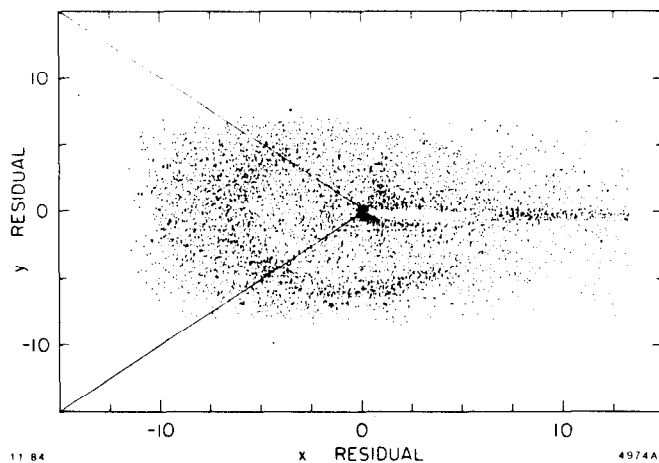


Fig. 6. Scatter plot of residuals from the beam track for approximately 200 beam tracks. The ring image was offset to get a clean count of photoelectrons in the left quadrant.

The measured and calculated results are shown in Table 1. The magnetic field has a small effect on the diffusion in the cooler mixture with isobutane but the effect is larger in methane alone. That the shrinkage is not as great as the calculated value for methane is probably due to systematic error that is not yet understood in the technique used.

Table 1

	Methane (70%) - Isobutane(30%)		Methane	
	(meas.)	(calc.)	(meas.)	(calc. or Ref. 4)
Field off	0.211		0.231	0.250
Field on	0.186		0.169	0.103
Ratio	0.88	0.82	0.73	0.41

8. Conclusion

The R & D results seen at SLAC are as follows:

- An NO of 50 has been measured for the short drift, TMAE-methane-isobutane detector. Ring images with 10 to 15 photoelectrons have been observed.
- Single electron attenuation lengths in methane(70%) - isobutane (30%) with 20 PPM oxygen have been measured to be 120 to 140 centimeters for 500 V/cm, corresponding to a life time of 30 to 40 microseconds. The lifetime in pure methane with 20 PPM oxygen is much longer.
- Longitudinal diffusion in methane-isobutane is 180 microns/cm^{1/2}, which results in a 1.5 mm error at 75 cm.
- Transverse diffusion is somewhat larger (230 microns/cm^{1/2}) for both methane and methane-isobutane(30%).
- A parallel magnetic field improves the transverse diffusion slightly with 30% isobutane and more dramatically with pure methane.

Acknowledgements

The authors acknowledge and express thanks for the valuable talents of Don McShurley, Robert Reif, Tom Weber and Henning Peterson for preparing the apparatus involved in these measurements and to Blair Ratcliff for valuable discussions.

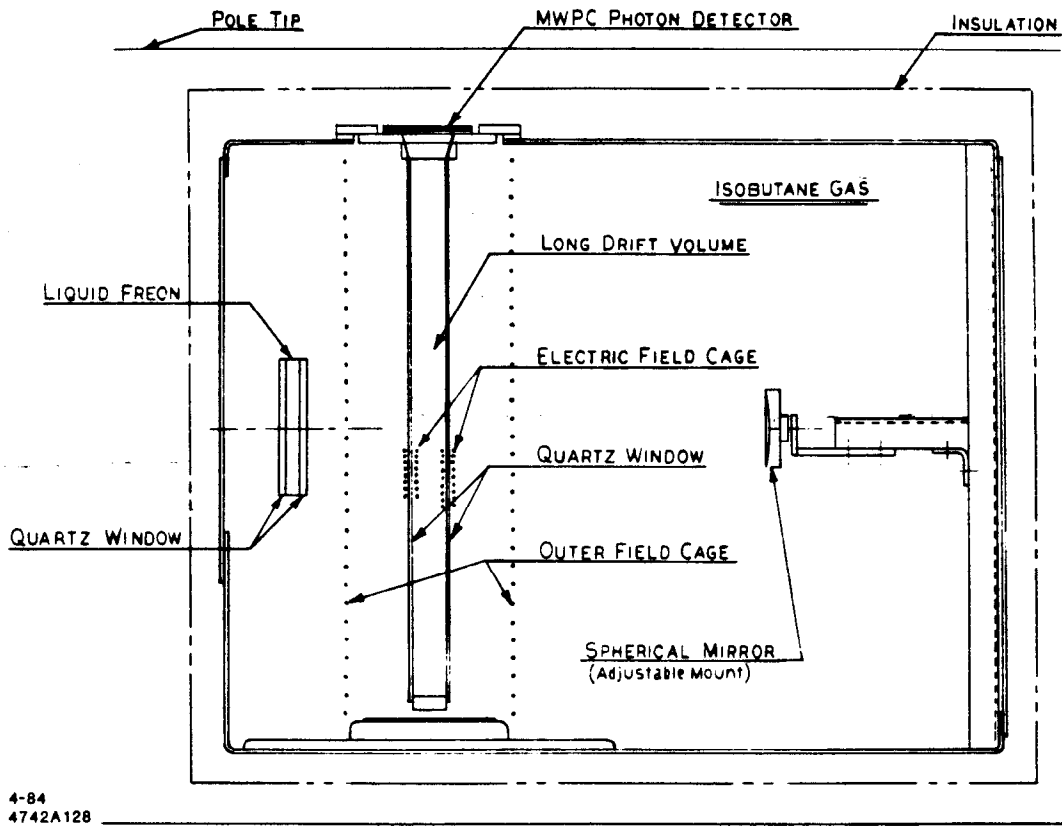


Fig. 7. The long drift box test device.

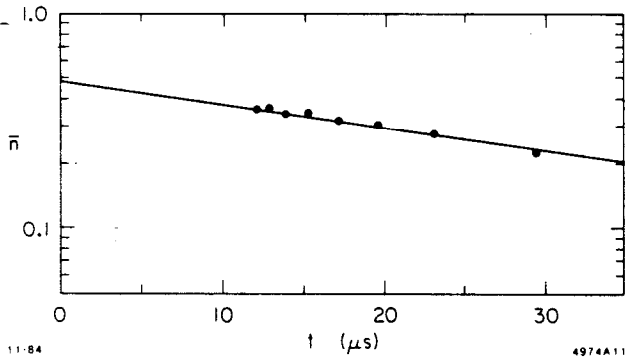


Fig. 8. Counting rate versus drift time for a fixed laser spot.

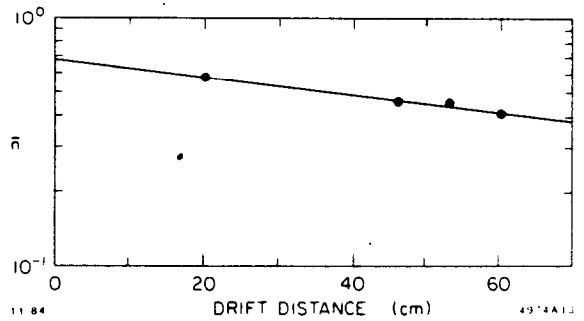


Fig. 10. Counting rate versus distance as the laser spot was moved along the drift direction.

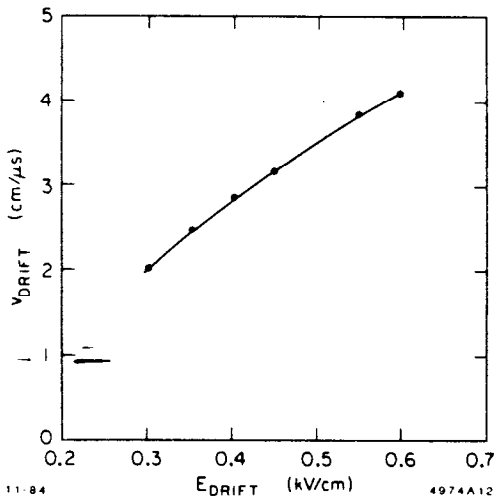


Fig. 9. Drift velocity versus electric field for methane (70%) - isobutane (30%) and 20 PPM oxygen.

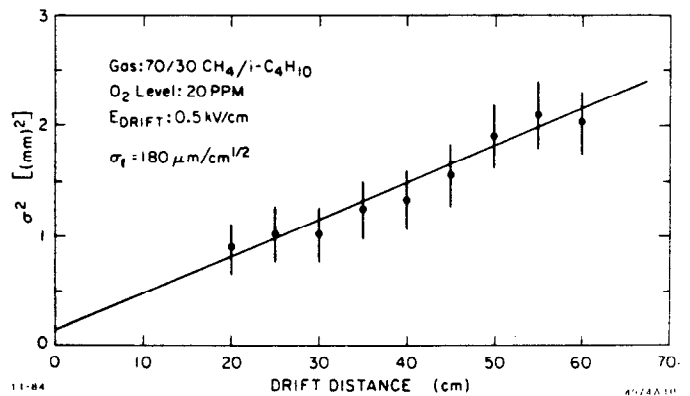


Fig. 11. Longitudinal diffusion versus drift distance.

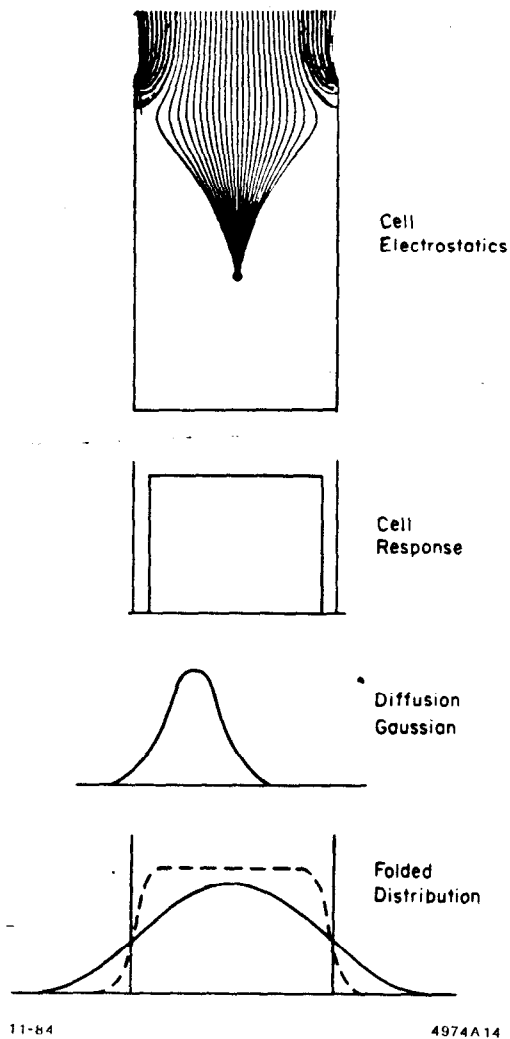


Fig. 12. (a) Cell electrostatic drift paths. (b) Cell profile of a single 4 MM cell in the multi-wire detector in the absence of diffusion. (c) Diffusion gaussian. (d) Cell profile after varying amounts of diffusion (c) are folded into the cell profile shown in (b).

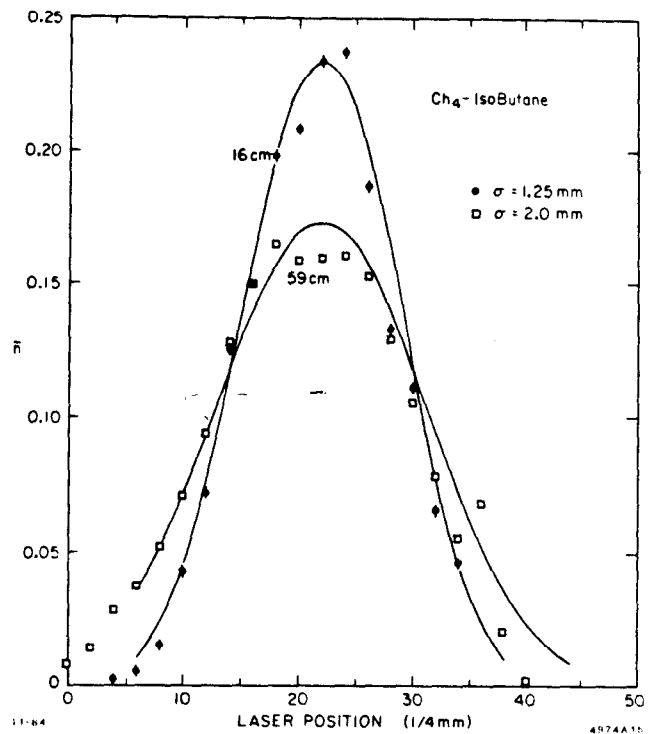


Fig. 13. Cell profiles measured with laser spot scanned across the detector in the long drift test device.

References

1. A. Roberts, Nucl. Instrum. Methods **9**, 55 (1960).
2. J. Seguinot and T. Ypsilantis, Nucl. Instrum. Methods **142**, 377(1977).
3. (a) DELPHI: CERN/LEPC/83-3, LEPC/P 2, 17 May 1983.
 (b) E-605: H Glass et al., Nucl. Sci. Symp. 1982:30 (IEEE Trans. **NS-30**, No. 1 February 1983).
 (c) LOGIC: B. Barish et al., CERN-LEP-LI-(6), January 1982, p. 28.
 (d) OMEGA: Bonn/Lancaster/Manchester/RAL/Sheffield. Proposal No. 231-Addendum 4, PPESP/82/24. M. Davenport et al., Nucl. Sci. Symp. 1982:30 (IEEE Trans. **NS-30**, No. 1, February 1983).
 (e) UA-2: RICH Collaboration (P. Baillon et al.), CERN / SPSC / 82-55, January 1982.
 (f) SLD: R. Baltrusaitis et al., SLC-LI-09, 1982, p. 59.
4. Nygren, PEP-198.